

MONTE CARLO SIMULATIONS WITH SYMANZIK'S IMPROVED ACTIONS IN THE LATTICE O(3) NON-LINEAR σ -MODEL

B BERG¹, S MEYER² and I. MONTVAY^{1,3}

Received 5 October 1983

The scaling properties of the lattice O(3) non-linear σ -model are studied. The mass-gap, energy momentum dispersion, correlation functions are measured by numerical Monte Carlo methods. Symanzik's tree-level and one-loop improved actions are compared to the standard (nearest neighbour) action.

1. Introduction

In the last few years considerable work was spent in Monte Carlo (MC) simulations of euclidean field theories. Sources of systematic errors and limitations to numerical simulations are:

- (a) statistical noise;
- (b) finite size effects;
- (c) finite lattice spacing effects.

Exact block-spin renormalization group transformations allow to simulate an L^d lattice on an $(L/n)^d$ lattice, where n^d (typically $n = 2$) is the block size and L a multiple of n . The lattice spacing on the new lattice is (na) in units of the lattice spacing a of the L^d lattice, and this transformation can, of course, be iterated. The price paid is the introduction of many new interactions, which in general cannot be calculated analytically. Monte Carlo renormalization group (MCRG) techniques [1, 2] use a truncated ansatz for the new interactions and try a numerical determination. In principle the above limitations (b) and (c) can be improved, but in practice statistical noise (a) is a severe problem. To the 2d O(3) non-linear σ -model Wilson's [2] MCRG version has been applied by Shenker and Tobochnik [3].

More recently Symanzik [4, 5] suggested a systematic procedure for constructing lattice actions, which minimize the cutoff dependence (c), and approach more rapidly the continuum limit. There are many possible actions on the lattice which formally converge to the same continuum limit when the lattice spacing $a \rightarrow 0$. In the

¹ II. Institut für Theoretische Physik der Universität Hamburg

² Fachbereich Physik der Universität Kaiserslautern; supported by Deutsche Forschungsgemeinschaft

³ Supported by Bundesministerium für Forschung und Technologie

case of renormalizable interactions, for small lattice spacing, a given action on the lattice is equivalent to a local theory on the continuum with a local effective lagrangian [4, 5]

$$\mathcal{L}_{\text{eff}} = \mathcal{L}_0 + a^2 \mathcal{L}_1 + a^4 \mathcal{L}_2 + \dots \quad (1.1)$$

\mathcal{L}_0 is the ordinary renormalizable continuum lagrangian in d dimensions, \mathcal{L}_1 contains operators of dimension $d + 2$, etc. Because of "irrelevant" operators the renormalization group equations contain non-universal scaling-violating terms. n -point Green functions calculated on the lattice obey

$$\left\{ -a \frac{\partial}{\partial a} + \bar{\beta}(g) \frac{\partial}{\partial g} + n\bar{\gamma}(g) \right\} G_n(p_1, \dots, p_n; g, a) = O(a^2 \ln a). \quad (1.2)$$

The suggestion of Symanzik is to choose the lattice action in such a way that the r.h.s. of eq. (2) is at most of order $O(a^4 \ln a)$. In the 2d $O(N)$ non-linear sigma model the improved action has the following form [4]:

$$\begin{aligned} S_{\text{imp}} = -g^{-1} a^2 \sum_j \left\{ & \left(-\frac{1}{2} \phi K \phi + J \phi \right) + a^2 J \left[c_1 \phi (\phi K \phi) + c_2 K \phi \right] + a^2 c_3 (J \phi)^2 \right. \\ & + a^2 c_4 J^2 + a^2 c_5 (K \phi)^2 + a^2 c_6 \sum_{\mu} \left[\partial_{\mu} \partial_{\mu}^{+} \phi \right]^2 \\ & + a^2 c_7 (\phi K \phi)^2 + a^2 c_8 \sum_{\mu} \left[\phi \partial_{\mu} \partial_{\mu}^{+} \phi \right]^2 \\ & \left. + a^2 c_9 \sum_{\mu\nu} \left[\frac{1}{2} (\partial_{\mu} + \partial_{\mu}^{+}) \phi \frac{1}{2} (\partial_{\nu} + \partial_{\nu}^{+}) \phi \right]^2 \right\}. \quad (1.3) \end{aligned}$$

Here the $O(N)$ vectors $\phi \equiv \phi_j$ on lattice sites j are normalized to unity: $\phi^2 = 1$, and the following notation is used:

$$\begin{aligned} \partial_{\mu} \phi_j &= a^{-1} (\phi_{j+\hat{\mu}} - \phi_j), & \partial_{\mu}^{+} \phi_j &= a^{-1} (\phi_j - \phi_{j-\hat{\mu}}), \\ K &= - \sum_{\mu=1}^2 \partial_{\mu} \partial_{\mu}^{+}. \end{aligned} \quad (1.4)$$

We often use $\beta = 1/g$.

The Green functions are obtained by differentiating $Z_{\text{imp}} = \int [d\phi] \exp(-S_{\text{imp}})$ with respect to the source vector J . The improved field, for instance, is

$$\phi_{j\alpha}^{\text{imp}} = \phi_{j\alpha} + c_1 \phi_{j\alpha} (\phi K \phi) + c_2 K \phi_{j\alpha}, \quad (1.5)$$

where α is the $O(N)$ index.

The improvement coefficients $c_i(g, N)$ can be determined in perturbation theory, in a $1/N$ expansion or, in principle, also by Monte Carlo checks of scaling (“trial and error”). For the standard action (SA) all coefficients c_i ($i = 1, \dots, 9$) are zero. The perturbatively tree-level improved action (TIA) has been calculated by Martinelli et al. [6]. Defining

$$c_i = c_i^0 + c_i^1 g + c_i^2 g^2 + \dots, \tag{1.6}$$

the tree-level result is

$$c_6^0 = -\frac{1}{24}, \tag{1.7}$$

and all other $c_i^0 = 0$. The TIA does not improve the 4-point functions to one-loop order. For comparison we note that Shenker and Tobochnik [3] performed a spin-wave fit to the block-spin renormalization group. They were led to the interaction term which we encounter for the TIA, however, with $c_6^0 = -\frac{1}{10}$.

Symanzik [5] has calculated the one-loop improved action (1LIA). One encounters in it two free parameters. We make here the same choice ($c_3^1 = c_7^1 = 0$) as in ref. [7], where also the relevant numerical integrals are explicitly given. For the convenience of the reader our final coefficients c_i^1 are listed in table 1. They differ slightly from those of ref. [5], but stay within the class of actions for which the improvement $O(a^2 \ln a) \rightarrow O(a^4 \ln a)$ of eq. (1.2) can be theoretically achieved. It is instructive to rewrite our 1LIA in the lattice notation

$$S = \sum_{i=1}^3 b_i S_i^b + \sum_{i=1}^{10} q_i S_i^q. \tag{1.8}$$

The first sum goes over all bilinear and the second sum over all quadrilinear

TABLE I
The coefficients c_i^1

i	c_i^1
1	-0 0048591
2	-0 0285844
3	0
4	-0 0023988
5	-0 0245659
6	-0 0032718
7	0
8	-0 0087486
9	+0 0194364

interaction terms. Coefficients, and interaction terms are listed in tables 2. The one-loop corrections to b_1 is notably large in the β region available for MC simulations.

MC simulations with the ILIA action were carried out in ref. [7], and for the TIA action by Falcioni et al. [8]. In the present paper we present more details and considerable extensions of the previous investigation [7]. We describe the used MC methods and summarize our statistics in sect. 2. Most of our results are obtained on a 50^2 lattice. In sect. 3 we present our continuum mass gap estimates and in sect. 4 we study the energy-momentum dispersion for states of momentum $K = 2\pi n/L$, $n = 0, 1, \dots, 10$. Sect. 5 contains our results for the magnetic susceptibility and a 4-point function. The latter is inconclusive because of statistical noise. We have also taken MC data for the two-point function at non-zero momenta. In the 2d $O(N)$ non-linear sigma model the $\bar{\beta}$ and $\bar{\gamma}$ functions of eq. (1.2) have universal (regularization scheme independent) parts [9]:

$$\bar{\beta}_{\text{univ}}(g) = -\frac{(N-2)}{2\pi}g^2 - \frac{(N-2)}{4\pi^2}g^3, \quad (1.9)$$

$$\bar{\gamma}_{\text{univ}}(g) = \frac{(N-1)}{2\pi}g. \quad (1.10)$$

The universal parts are obtained from a 2-loop calculation in any regularization. Continuum estimates of the mass gap (cf. sect. 3) use the Λ scale as obtained from

TABLE 2
(a) Coefficients of bilinear interactions

b_i	S_i^b	i
$0.4892 g + \frac{4}{3}$	$\phi_j \phi_{j+\hat{\mu}}$	1
$-0.0945 g - \frac{1}{12}$	$\phi_j \phi_{j+2\hat{\mu}}$	2
$-0.0983 g$	$\phi_j \phi_{j+\hat{\mu}+\hat{\nu}}, \quad (\mu \neq \nu)$	3

(b) Coefficients of quadrilinear interactions

q_i	S_i^q	i
$-0.0175 g$	$(\phi_j \phi_{j+\hat{\mu}})^2, \quad (\phi_j \phi_{j+\hat{\mu}})(\phi_j \phi_{j-\hat{\mu}}),$	1,2
	$(\phi_j \phi_{j+\hat{\mu}})(\phi_{j+\hat{\mu}} \phi_{j+2\hat{\mu}})$	3
$+0.0194 g$	$(\phi_j \phi_{j+2\hat{\mu}})^2, \quad (\phi_j \phi_{j+\hat{\mu}+\hat{\nu}})^2,$	4,5
	$-(\phi_j \phi_{j+\hat{\mu}+\hat{\nu}})(\phi_j \phi_{j-\hat{\mu}-\hat{\nu}}),$	6,7
	$-(\phi_j \phi_{j+\hat{\mu}+\hat{\nu}})(\phi_{j+\hat{\mu}+\hat{\nu}} \phi_{j+2\hat{\mu}}),$	8
	$(\phi_j \phi_{j+\hat{\mu}+\hat{\nu}})(\phi_{j+\hat{\mu}-\hat{\nu}} \phi_{j+2\hat{\mu}}),$	9
	$(\phi_j \phi_{j+\hat{\mu}+\hat{\nu}})(\phi_{j-\hat{\mu}+\hat{\nu}} \phi_{j+2\hat{\mu}}),$	10
	$(\mu \neq \nu)$	

the universal $\bar{\beta}$ function, and try to establish a scaling window (cf. ref. [10] for a more detailed discussion). We will call this *asymptotic scaling* (valid for $g, a \rightarrow 0$ asymptotically). More generally *scaling* means: eq. (1.2) holds with some function $\bar{\beta}(g)$ and the r.h.s. = 0. Scaling but not necessarily asymptotic scaling is improved by using Symanzik actions. Even if scaling holds, higher perturbative (3-loop, ...) corrections to the $\bar{\beta}$ and $\bar{\gamma}$ functions could spoil asymptotic scaling in an intermediate coupling constant range. In mass ratios (or other dimensionless quantities) these perturbative corrections drop out, and we expect improvement. For instance in the equation

$$\frac{m_1}{m_2} = \text{const} \cdot \{1 + O(a^2 \ln a)\},$$

the correction on the r.h.s. is improved to $O(a^4 \ln a)$.

In sect. 6 we analyse our results with respect to scaling in the sense of eq. (1.2). This is enabled by the fact that we have measured a considerable number of higher-momentum states. In sect. 7 we summarize our results and draw some conclusions.

2. The Monte Carlo statistics

In this section we summarize our MC data. A review of the MC method is given in ref. [11]. For bilinear (spin) interactions the heat bath method is very efficient. Upgrading of a spin $s = s_j$ amounts to replacing it by a new spin s' which is selected with the probabilistic Boltzmann weight

$$e^{\beta s' S}, \quad S = \sum_j a_j \phi_j, \quad (2.1)$$

where the sum involves all spins interacting with s . More precisely sS is the contribution of spins involving s to the total action.

In our investigation we have used the heat bath method for the SA and the TIA. For the SA S is a sum of four terms and for the TIA S is a sum of eight terms. As most of the computer time is spent in calculating S with the weight (2.1), upgrading the TIA is only slightly (~ 1.2) slower than upgrading the SA.

In the case of 1LIA the quadrilinear interaction terms (cf. table 2b) prevent us from applying the heat bath method. We have used Metropolis with 4 hits per trial. The upgrading procedure is roughly 5 times slower than for the SA. We perform measurements of all considered observables after each sweep. A sweep consists in upgrading each spin of the lattice once in the mean; we did random upgrading (cf. ref. [10], subsect. 2.1). For all three actions, measurements take about the same time. In the case of 1LIA, measurements took roughly $\frac{1}{3}$ of the used computer time, one

TABLE 3
(a) E and statistics for the SA

β	E	sweeps
0.4	0.1366 ± 0.0002	9 000
0.8	0.2920 ± 0.0001	18 200
0.9	0.3351 ± 0.0001	18 200
1.0	0.3801 ± 0.0002	18 200
1.1	0.4264 ± 0.0002	18 200
1.2	0.4728 ± 0.0003	18 200
1.3	0.5188 ± 0.0003	18 200
1.4	0.5621 ± 0.0003	15 400
1.5	0.6016 ± 0.0002	18 000
1.6	0.6364 ± 0.0003	18 200
1.8	0.6886 ± 0.0002	16 100
100 ² lattice:		
1.4	0.5620 ± 0.0001	20 800
1.5	0.6016 ± 0.0002	21 200

(b) E and statistics for the TIA

β	E	sweeps
0.8	0.3820 ± 0.0002	15 400
0.9	0.4349 ± 0.0002	14 600
1.0	0.4879 ± 0.0002	18 000
1.1	0.5382 ± 0.0002	18 000
1.2	0.5852 ± 0.0003	18 000
1.25	0.6068 ± 0.0004	18 000
METROPOLIS		
0.8	0.3817 ± 0.0002	18 000

(c) E and statistics for the 1LIA

β	E	sweeps
0.6	0.3950 ± 0.0003	22 200
0.7	0.4424 ± 0.0004	18 000
0.8	0.4812 ± 0.0002	21 900
0.9	0.5362 ± 0.0009	21 000
1.0	0.5834 ± 0.0007	18 000
1.1	0.6297 ± 0.0011	31 800

sweep and measurements is only by a factor 2.5 slower than for the SA. The Metropolis upgrading is, however, clearly less efficient than heat bath upgrading, therefore the error bars are larger.

Together with mean values for the average link action

$$E \stackrel{\text{def}}{=} \langle 1 - \phi_j \phi_{j+\hat{\mu}} \rangle, \quad (2.2)$$

our final statistics is collected in table 3. At the beginning we did always 2000 sweeps without measurements, for reaching equilibrium. At identical β values the results for E are clearly distinct for the three different actions; in particular TIA and 1LIA are notably different. We always calculate our error bars by dividing our complete statistics into 10 bins. Typically this amounts to groups of 2000 events. For the SA at $\beta = 1.4, 1.5$ we have also results on a 100^2 lattice. All other calculations were done on a 50^2 lattice. At $\beta = 0.8$ we have also used the Metropolis upgrading for the TIA and checked it against results with the heat bath upgrading. Within statistical errors we found perfect agreement.

3. The mass gap

In this section we present our results for the mass gap. We also compare with previously reported mass gap estimates [3, 12–17].

We obtain upper bounds on the mass gap from correlations between momentum zero eigenstates

$$c(\Delta t) = \langle \tilde{\phi}(t) \tilde{\phi}(t + \Delta t) \rangle, \quad (3.1)$$

where

$$\tilde{\phi}(t) = \sum_{x=0}^{L-1} \phi(x, t). \quad (3.2)$$

In the case of 1LIA, the improved field (1.5) is taken. For our analysis we use the mass gap definition

$$m(\Delta t) = -\frac{1}{\Delta t} \ln \left| \frac{c(\Delta t)}{c(0)} \right|, \quad (\Delta t = 1, 2, \dots). \quad (3.3)$$

In the case of nearest-neighbour interactions, we have a transfer matrix T , which connects nearest neighbour time-planes. If the transfer matrix is bounded from below (not necessarily positive definite), we obtain upper bounds on the mass gap from the MC values for $m(\Delta t)$. If the transfer matrix is positive definite $m(\Delta t)$,

$\Delta t \rightarrow \infty$ will decrease monotonically against the real mass gap. Otherwise oscillations due to complex eigenvalues of the transfer matrix are possible. In the latter case it is dangerous to use the mass gap definitions (cf. for instance ref. [10])

$$\hat{m}(\Delta t_1, \Delta t_2) = -\frac{1}{\Delta t_2 - \Delta t_1} \ln \frac{c(\Delta t_2)}{c(\Delta t_1)},$$

$$(\Delta t_1, \Delta t_2 = 1, 2, \dots; \Delta t_2 > \Delta t_1).$$

For the TIA and 1LIA one has to generalize the concept of the transfer matrix, because of next-nearest neighbour interactions. Now also next-neighbour time-planes become connected and we can trust $m(\Delta t)$ to be an upper bound only for $\Delta t \geq 2$. This is not an academic question, as for the TIA the $m(1)$ value is in general the lowest.

Our MC results rely on the statistics outlined in sect. 2. We have measured all possible correlations, this means $t = 0, 1, \dots, \frac{1}{2}L$, ($L = 50, 100$). To illustrate our

TABLE 4
Correlation functions at selected values of β

Δt	$\beta = 1.2, SA$	$\beta = 1.6, SA$	$\beta = 1.1, TIA$	$\beta = 0.8, 1LIA$
0	3.431 ± 0.023	11.4 ± 0.2	4.125 ± 0.027	3.056 ± 0.016
1	2.504 ± 0.023	10.7 ± 0.2	3.278 ± 0.027	1.779 ± 0.015
2	1.833 ± 0.023	10.2 ± 0.2	2.534 ± 0.025	1.136 ± 0.015
3	1.341 ± 0.022	9.6 ± 0.2	1.948 ± 0.024	0.657 ± 0.015
4	0.981 ± 0.020	9.1 ± 0.2	1.489 ± 0.021	0.381 ± 0.016
5	0.719 ± 0.018	8.7 ± 0.3	1.131 ± 0.019	0.229 ± 0.016
6	0.529 ± 0.016	8.3 ± 0.3	0.852 ± 0.019	0.132 ± 0.014
7	0.389 ± 0.014	7.9 ± 0.3	0.634 ± 0.018	0.081 ± 0.011
8	0.286 ± 0.012	7.6 ± 0.3	0.464 ± 0.018	0.050 ± 0.009
9	0.214 ± 0.010	7.3 ± 0.3	0.334 ± 0.018	0.030 ± 0.007
10	0.162 ± 0.010	7.0 ± 0.3	0.239 ± 0.021	0.021 ± 0.007
11	0.123 ± 0.011	6.8 ± 0.3	0.169 ± 0.023	0.011 ± 0.007
12	0.095 ± 0.011	6.5 ± 0.3	0.117 ± 0.026	0.010 ± 0.008
13	0.074 ± 0.011	6.3 ± 0.3	0.081 ± 0.028	0.005 ± 0.009
14	0.059 ± 0.010	6.1 ± 0.3	0.057 ± 0.029	0.003 ± 0.009
15	0.044 ± 0.010	6.0 ± 0.3	0.043 ± 0.030	0.000 ± 0.012
16	0.030 ± 0.011	5.8 ± 0.3	0.032 ± 0.032	0.004 ± 0.011
17	0.017 ± 0.012	5.7 ± 0.3	0.026 ± 0.035	0.006 ± 0.011
18	0.008 ± 0.014	5.5 ± 0.3	0.022 ± 0.038	0.003 ± 0.010
19	0.001 ± 0.016	5.4 ± 0.4	0.021 ± 0.041	0.001 ± 0.011
20	-0.007 ± 0.018	5.3 ± 0.4	0.023 ± 0.043	0.003 ± 0.011
21	-0.013 ± 0.020	5.3 ± 0.4	0.029 ± 0.046	-0.002 ± 0.012
22	-0.016 ± 0.021	5.2 ± 0.4	0.036 ± 0.049	-0.005 ± 0.013
23	-0.015 ± 0.023	5.2 ± 0.4	0.041 ± 0.051	-0.007 ± 0.013
24	-0.013 ± 0.024	5.2 ± 0.4	0.044 ± 0.052	-0.007 ± 0.014
25	-0.014 ± 0.024	5.1 ± 0.4	0.046 ± 0.052	-0.009 ± 0.015

method for extracting the mass gap, we give in table 4 all calculated correlations for some selected values of β . Table 5 contains the $m(\Delta t)$ mean values, which are obtained from these correlations. In case of the 1LIA we have taken the correlations of the improved field (1.5). For the final results error bars are calculated (by the method of sect. 2) from the error bars of the relevant $C(\Delta t)$, neglecting the error bar of $C(0)$ because of correlations. For large Δt the error bars of $C(\Delta t)$ increase and finally reliable results can no longer be obtained.

The values $m(\Delta t)$ ($\Delta t = 1(2), \dots, \frac{1}{2}L$) are upper bounds for the mass gap. As long as $m(\Delta t)$ is rather stable when going to larger values Δt , we hope to obtain a good approximation to the mass gap (at the β value in question). If the correlation length ξ becomes too large, we enter (on a finite lattice) the spin-wave region, and no sensible value for the mass gap can be extracted. In this case a power law behaviour is indicated for the correlation function $C(\Delta t)$, $\Delta t \rightarrow \infty$ by strongly decreasing values for $m(\Delta t)$ as $\Delta t \rightarrow \infty$. For the SA on the 50^2 lattice we illustrate this at $\beta = 1.6$, where the correlation length is $\xi \cong 20$.

TABLE 5
Mass-gap estimates (mean values) from the correlations of table 4

Δt	$\beta = 1.2, SA$	$\beta = 1.6, SA$	$\beta = 1.1, TIA$	$\beta = 0.8, 1LIA$
1	0.315	0.063	0.23	0.54
2	0.313	0.056	0.24	0.50
3	0.313	0.057	0.25	0.51
4	0.313	0.056	0.25	0.52
5	0.313	0.054	0.26	0.52
6	0.312	0.053	0.26	0.52
7	0.311	0.052	0.27	0.52
8	0.311	0.051	0.27	0.51
9	0.308	0.050	0.28	0.51
10	0.305	0.049	0.28	0.50
11	0.302	0.047	0.29	0.51
12	0.298	0.047	0.30	0.48
13	0.294	0.046	0.30	
14	0.290	0.045	0.30	
15	0.291	0.043	0.30	
16	0.296	0.042		
17	0.312	0.041		
18		0.040		
19		0.039		
20		0.038		
21		0.036		
22		0.036		
23		0.034		
24		0.033		
25		0.032		

Our final mass gap results are summarized in fig. 1. The Λ parameters of this figure are defined by $(\beta = \beta_S, \beta_{TI}, \beta_{LII})$

$$\Lambda_L^{S,I} = 2\pi\beta \exp(-2\pi\beta)(1 + O(1/\beta)), \tag{3.4}$$

S = standard, I = improved. The $O(g)$ coefficients, distinguishing TIA and 1LIA, do not affect the asymptotic Λ scale, Λ_L^I . The full lines of fig. 1 are approximate continuum estimates. For the TIA the full line is taken from ref. [8], and our MC data are seen in good agreement with it. For the SA we have taken a value which is consistent with previous MC literature [3,12-14]. In this case the discrepancies in the literature are, however, large and the status of asymptotic scaling is now obscured by ref. [14].

In fig. 2 we plot the defects

$$d = \text{const} \frac{m}{\Lambda_L^{S,I}}, \tag{3.5}$$

versus $\ln \xi$, where ξ is the correlation length. (The constants in (3.5) are adjusted such that always $d(\beta = 0.8) = 1.0$.) We clearly find improvement in the sense that the mass gap exhibits asymptotic scaling already at a very small correlation length

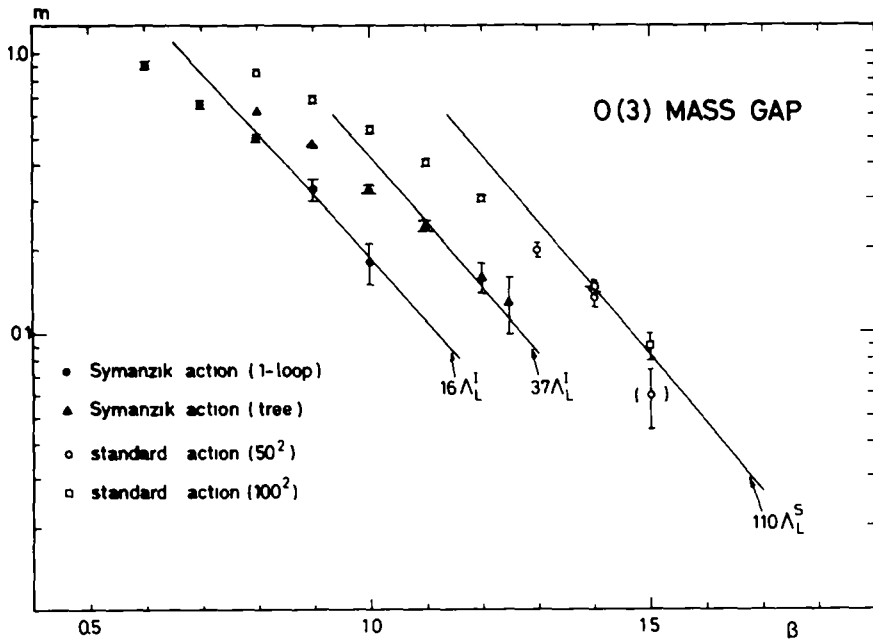


Fig 1 The mass gap

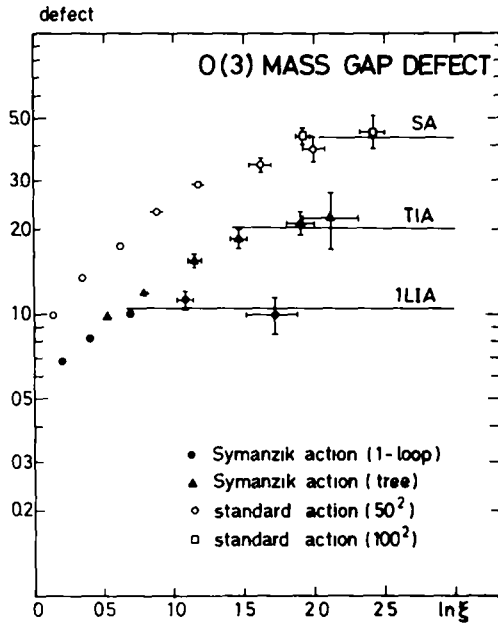


Fig 2 The mass-gap defect.

for the 1LIA. For the SA we have on a lattice of the same size (50^2) no signal at all for asymptotic scaling. To some extent this result is a surprise, because Symanzik's improvement is concerned with scaling and not (at least directly) with asymptotic scaling. In table 6 we roughly estimate the correlation length at the beginning ξ_{begin} and end ξ_{end} of the scaling windows for our three actions on a 50^2 lattice. The end of the scaling windows is due to finite-size effects: lattice size and (related) spin-wave problems. The practical improvement is measured by the fraction $q = \xi_{begin}/\xi_{end}$. We have $q \approx 2.5$ (1LIA), $q \approx 2.0$ (TIA) and $q \approx 1.0$ (SA). For the 1LIA asymptotic scaling sets in at the very small correlation length $\xi_{begin} \approx 2$, but we pay with early finite-size effects at $\xi_{end} \approx 5$. Consequently, for the practical purposes of a mass gap calculation the TIA seems to be similarly useful as the 1LIA, in particular because the heat-bath method is applicable for the TIA. On the other hand, both

TABLE 6
Asymptotic scaling windows on a 50^2 lattice

	ξ_{begin}	ξ_{end}
SA	7	7
TIA	4	8
1LIA	2	5

improved actions provide clearly a practical improvement as compared with the SA. For the SA asymptotic scaling can (if at all) only be seen on lattices of size $\geq 100^2$ and therefore the MC calculations are much more time consuming.

The ratio Λ_L^I/Λ_L^S has been calculated analytically [5, 8, 18, 19] for the $O(N)$ sigma model and the $O(3)$ result is

$$\Lambda_L^I/\Lambda_L^S = 2.219. \quad (3.6)$$

The MC simulation, however, gives

$$\Lambda_L^I/\Lambda_L^S \approx 3.0, \quad (\text{from TIA versus SA}), \quad (3.7a)$$

$$\Lambda_L^I/\Lambda_L^S \approx 6.9, \quad (\text{from 1LIA versus SA}). \quad (3.7b)$$

Particularly notable is the large difference between TIA and 1LIA. This is argued to be due to perturbative (3-loop etc.) corrections to the Λ -scale (3.4). We can easily imagine asymptotic convergence of the full lines in fig. 1 by a small deviation in their slope, which cannot be numerically detected in the small scaling windows. Assuming the 1LIA estimate to be the best, a qualitative figure of the expected scaling curves was given in ref. [19]. The 1LIA gives a result rather close to Lüscher's [16] estimate, which is based on a new finite-volume method. Lüscher's value is conjectured to be very close to the exact mass-gap result. Strong-coupling estimates [15] are between TIA and SA (closer to TIA), and finally also variational calculations [17] seem to approach a point, where estimates become possible.

4. The energy-momentum dispersion

In our investigation we have also measured correlations between momentum $K = 0, \pm 2\pi n/L$ ($n = 1, \dots, [\frac{1}{2}L]$) eigenstates. These correlations are defined by

$$C(K, \Delta t) = \text{Re}\{\langle \tilde{\phi}(K, t) \tilde{\phi}(K, t + \Delta t) \rangle\}, \quad (4.1)$$

TABLE 7
Correlations for $K = \frac{14}{50}\pi$ eigenstates

Δt	SA, $\beta = 1.0$	TIA, $\beta = 0.8$	1LIA, $\beta = 0.6$
0	1.220 \pm 0.002	1.279 \pm 0.002	2.82 \pm 0.02
1	0.458 \pm 0.002	0.502 \pm 0.002	-0.56 \pm 0.01
2	0.172 \pm 0.001	0.171 \pm 0.002	0.17 \pm 0.01
3	0.065 \pm 0.001	0.056 \pm 0.001	0.08 \pm 0.01
4	0.026 \pm 0.001	0.018 \pm 0.001	0.01 \pm 0.01
5	0.011 \pm 0.001	0.006 \pm 0.001	-0.01 \pm 0.01
6	0.004 \pm 0.001	0.002 \pm 0.001	

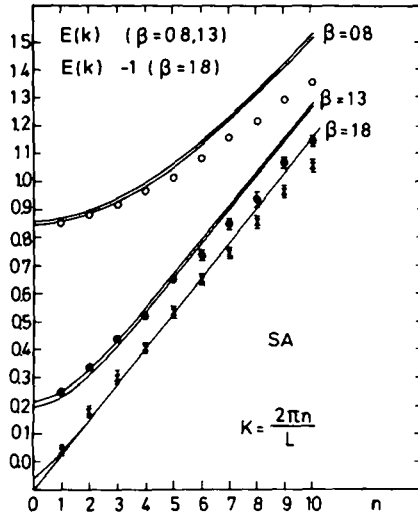


Fig 3 Energy-momentum dispersion for the SA

where

$$\tilde{\phi}(K, t) = \sum_{x=0}^{L-1} e^{iKx} \phi(x, t),$$

and in case of the 1LIA again the improved field (1.5) is taken. For practical reasons (disk space) we have only considered $n = \pm 1, \pm 2, \dots, \pm 10$. Having in mind a check of the relativistic energy-momentum dispersion, i.e. the restoration of Lorentz

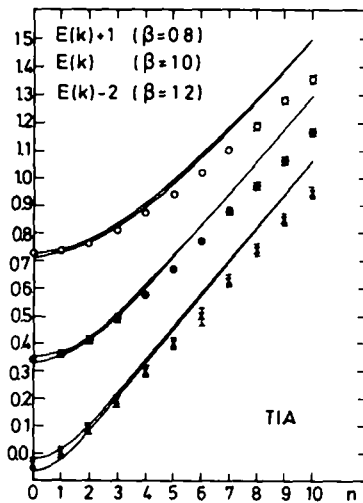


Fig 4 Energy-momentum dispersion for the TIA

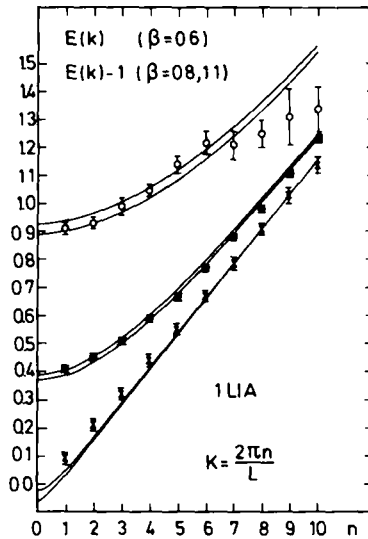


Fig 5 Energy-momentum dispersion for the 1LIA

invariance

$$E(K) = \sqrt{m^2 + K^2}, \quad (4.2)$$

these values are the most important. From our MC data for the correlations (4.1) we note a tendency of the Fourier transform to suppress statistical noise. This may have importance for attempts to improve mass-gap estimates. In table 7 we give the correlation functions for $K = \frac{1}{50}\pi$ at one value of β for each action. Notable is the strong oscillation in the case of the 1LIA at short distances.

Previously the energy-momentum dispersion (4.2) has been investigated within a variational approach (cf. ref. [17] and references given there). In figs. 3–5 our results are summarized. We find no improvement by going from the SA to the TIA, but considerable improvement of the energy-momentum dispersion for the 1LIA. We attribute this to the off-diagonal terms of the 1LIA (cf. table 2a), which are important for improving rotation invariance.

5. Correlation functions

In the previous sections we have considered the mass-gap and momentum eigenstates. Other examples for quantities satisfying the RG equation (1.2) are 2-

and 4-point functions

$$S_2 = \left. \frac{\delta^2 Z[J]}{\delta J_1 \delta J_2} \right|_{J=0}, \tag{5.1}$$

$$S_4 = \left. \frac{\delta^4 Z[J]}{\delta J_1 \delta J_2 \delta J_3 \delta J_4} \right|_{J=0}. \tag{5.2}$$

The 2-point function at zero 2-momentum is the magnetic susceptibility

$$\chi_m = S_2(p_1 = p_2 = 0). \tag{5.3}$$

It is supposed to scale like [9]

$$\chi_m = C(2\pi\beta)^{-4} \exp(4\pi\beta)(1 + O(1/\beta)). \tag{5.4}$$

For the SA large scaling deviations in χ_m were found in refs. [20,21]. Our present results are given in table 8. For the SA and the TIA they are consistent with the previous literature [8,20,21]. In fig. 6 the defect $\delta_m = \beta^4 \exp(-4\pi\beta)\chi_m$ is plotted. We find a window consistent with asymptotic scaling only for the ILIA. This leads to the estimate

$$C \approx 0.3. \tag{5.5}$$

TABLE 8
Magnetic susceptibilities

SA		TIA	
β	χ_m	β	χ_m
04	1 80 ± 0 03	08	7 7 ± 0 2
08	4.59 ± 0 08	09	10 9 ± 0 4
09	6 35 ± 0 14	10	18 7 ± 0 6
10	9 28 ± 0 30	11	31 7 ± 1 2
11	13 4 ± 0 4	12	64 6 ± 5 1
12	22 1 ± 0 6	125	97 0 ± 12 0
13	42 8 ± 3 0		METROPOLIS.
14	84 0 ± 5 0	08	7 4 ± 0 2
15	181 0 ± 14 0		
16	350 0 ± 13 0		
18	687 0 ± 10 0		
	100 ² lattice		ILIA
14	70 1 ± 4 7	β	χ_m
15	171 0 ± 20 0	06	5 42 ± 0 14
		07	8 19 ± 0 26
		08	12 1 ± 0 4
		09	22 9 ± 2 2
		10	50 0 ± 8 0
		11	193 0 ± 43.0

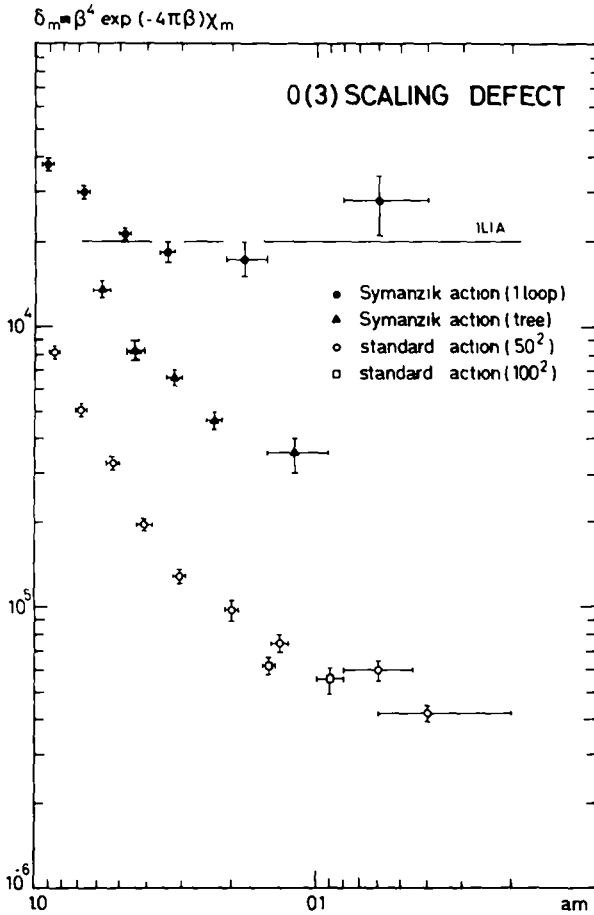


Fig 6 Scaling defect for the magnetic susceptibility

For the SA and TIA estimates of C have to involve more hand-waving arguments. Dependence of asymptotic scaling for χ_m on the choice of the lattice action was also reported in ref. [22].

Finally we have also measured the “generalized susceptibility”

$$\chi_4 = \frac{S_4(p_1 = p_2 = p_3 = p_4 = 0)}{\chi_m^2}, \tag{5.6}$$

which has no wave-function renormalization. On our rather large lattice the results were, however, compatible with statistical noise. For the SA and TIA data on smaller lattices were presented in [8].

6. Scaling behaviour of the mass-gap and two-point function

As discussed in the introduction, scaling (in general) means the validity of the RG equation (1.2) with some functions $\bar{\beta}(g)$ and $\bar{\gamma}(g)$ satisfying for $g \rightarrow 0$

$$\begin{aligned} \bar{\beta}(g) &\rightarrow \bar{\beta}_{\text{univ}}(g) + O(g^4), \\ \bar{\gamma}(g) &\rightarrow \bar{\gamma}_{\text{univ}}(g) + O(g^2). \end{aligned} \tag{6.1}$$

(The regularization-independent, universal parts $\bar{\beta}_{\text{univ}}, \bar{\gamma}_{\text{univ}}$ are given by eqs. (1.9)-(1.10).) In the present section we shall be concerned with ‘‘RG-invariant’’ functions which do not depend on wave-function renormalization and hence on $\bar{\gamma}(g)$. Let us denote such a quantity, having mass dimension D , by F_D . In a lattice calculation physical quantities occur in ‘‘lattice units’’, that is the dimensionless function $f_D = a^D F_D$ is available (a = lattice spacing). This function can depend, in general, on different physical parameters (measured in lattice units) like e.g. $L/a = N$ (L = lattice size), $r/a = n$ (r = distance), $ap = 2\pi\nu/N$; $\nu = 0, \pm 1, \dots$ (p = momentum)* or $aT = N_\tau^{-1}$ (T = temperature) etc. From the RG-equation

$$\left[-a \frac{\partial}{\partial a} + \bar{\beta}(g) \frac{\partial}{\partial g} \right] F_D = 0, \tag{6.2}$$

it follows for

$$\begin{aligned} f_D &= f_D(g, N, n, \nu, N_\tau) = a^D F_D, \\ \left[D + N \frac{\partial}{\partial N} + n \frac{\partial}{\partial n} - \nu \frac{\partial}{\partial \nu} + N_\tau \frac{\partial}{\partial N_\tau} + \bar{\beta}(g) \frac{\partial}{\partial g} \right] f_D &= 0. \end{aligned} \tag{6.3}$$

Note, that here the variables N, n, ν, \dots are considered as continuous, although on a lattice they are, of course, discrete (integer). This means that in a lattice calculation the derivatives have to be approximated by difference quotients. In the continuum limit this approximation can, however, be made arbitrarily good by using a high-order interpolation between the values obtained at neighbouring integers. As a simple example for the physical quantity F_D , let us consider the mass gap m_G with $D = 1$. The RG equation (6.3) for $\mu_G = am_G$ is

$$\left[1 + \bar{\beta}(g) \frac{\partial}{\partial g} \right] \mu_G(g) = 0. \tag{6.4}$$

This can be used for the calculation of the lattice β -function:

$$\bar{\beta}(g) = - \frac{\mu_G}{d\mu_G/dg} = - \left(\frac{d \ln \mu_G}{dg} \right)^{-1}. \tag{6.5}$$

* Here we assume periodic boundary conditions

Note that in these equations the volume dependence of the mass gap is neglected, that is the lattice size is assumed to be very much larger than the relevant correlation length ("infinite-volume limit").

Other examples for the quantities satisfying the RG equation (6.3) can be obtained from the 2- and 4-point functions (5.1), (5.2). The "generalized susceptibility" χ_4 defined in (5.6) has no wave-function renormalization, it is dimensionless and it can depend only on the volume. On the lattice it satisfies the RG equation

$$\left[N \frac{\partial}{\partial N} + \bar{\beta}(g) \frac{\partial}{\partial g} \right] \chi_4(g, N) = 0. \quad (6.6)$$

This can, in principle, also be used to determine $\bar{\beta}(g)$, but χ_4 is rather difficult to measure numerically. Therefore, we considered the normalized two-point function as a function of the momentum

$$R_2 = \frac{S_2(ap)}{S_2(ap=0)} = \frac{S_2(ap)}{\chi_m}. \quad (6.7)$$

(Here ap is some component of the lattice momentum having the values $ap = 2\pi\nu/N$; $\nu = 0, \pm 1, \pm 2, \dots$.) According to eq. (6.3) and neglecting the volume dependence, R_2 satisfies

$$\left[-\nu \frac{\partial}{\partial \nu} + \bar{\beta}(g) \frac{\partial}{\partial g} \right] R_2(g, \nu) = 0. \quad (6.8)$$

This implies

$$\bar{\beta}(g) = \frac{\partial R_2 / \partial \ln \nu}{\partial R_2 / \partial g}. \quad (6.9)$$

Measuring the two-point function R_2 at different values of g and ν allows, therefore, a numerical determination of the lattice $\bar{\beta}$ -function.

The equations like (6.6) or (6.8) imply that the functions χ_4 and R_2 depend only on a particular combination of the two arguments. For instance, the solution of eq. (6.8) is, with an arbitrary function $r_2(x)$,

$$R_2 = r_2 \left(\ln \nu + \int^g \frac{dg'}{\bar{\beta}(g')} \right). \quad (6.10)$$

This property can be easily checked graphically. A convenient choice is to plot $\ln R_2$ as a function of $\ln(ap)$ and to try to bring the curves belonging to the different coupling constant values on top of each other by a shift in $\ln(ap)$. If this can be achieved there is scaling, the obtained universal curve is the continuum $\ln R_2$

function and the lattice $\bar{\beta}$ -function can also be extracted from the shifts. The result of this procedure for the case of the SA and 1LIA is shown on figs. 7, 8. As it can be seen, the result is a rather nice scaling curve, in spite of the large violations of asymptotic scaling observed for the SA in previous sections. There are, of course, also small scaling violations seen in fig. 7 but the corresponding curve for the 1LIA (and also for TIA) is so similar, that one cannot draw an immediate conclusion concerning the quality of scaling in the three cases. The crucial question is, whether the lattice $\bar{\beta}$ -function obtained from the normalized 2-point function R_2 is universal (as it should be), that is whether it describes the scaling behaviour of all the quantities in the theory.

In order to study these questions quantitatively, we numerically determined the lattice $\bar{\beta}$ -function for all the three actions using eqs. (6.5) and (6.9). The derivatives were estimated from a quadratic interpolation using the two neighbouring values in g and $\ln \nu$. The obtained results are collected in table 9. As it can be seen, the lattice $\bar{\beta}$ -function for SA is rather different from the asymptotically valid universal part (1.9) even at the smallest measured values of the coupling g . This explains the observed large deviations from asymptotic scaling. The 1LIA comes at $g^{-1} = \beta = 0.9$

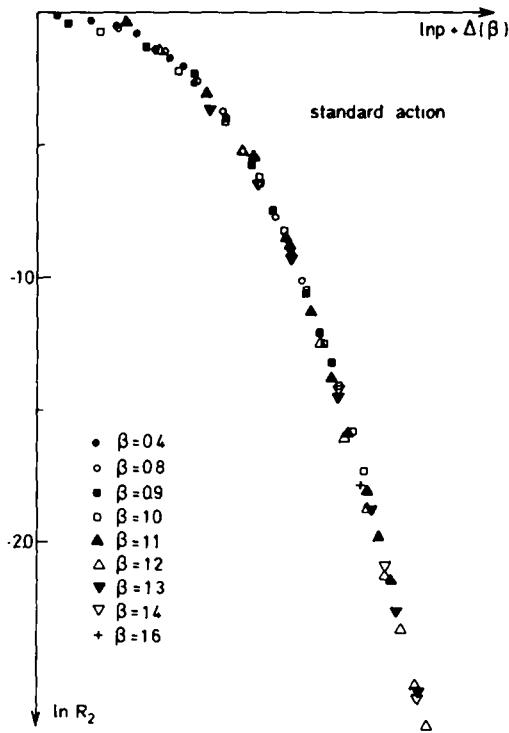


Fig. 7. Test of scaling for the SA.

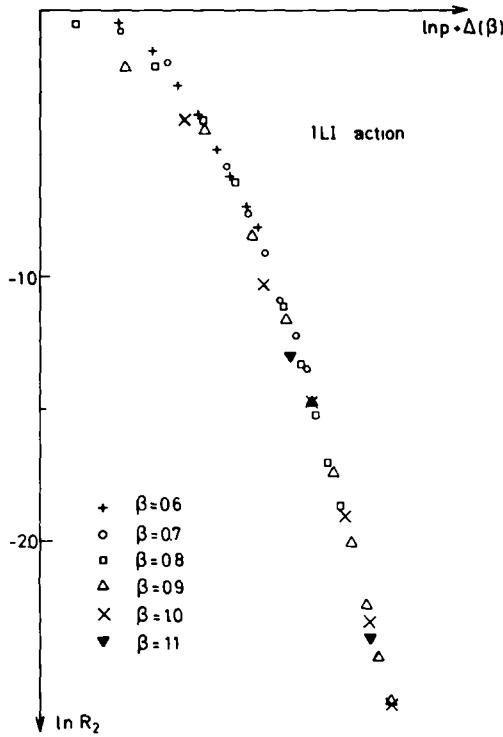


Fig 8. Test of scaling for the 1LIA

rather near to $\bar{\beta}_{umiv}$ (it actually coincides with $\bar{\beta}_{umiv}$ within errors). The TIA is between SA and 1LIA. The universality of the $\bar{\beta}$ -function values, obtained from the mass gap and from different momenta, is very good at $\beta = 0.9$ for the 1LIA and at $\beta = 1.2$ for the TIA. In the other points the numbers are in most cases compatible with universality within errors. An exception is $\beta = 0.9$ for the SA and perhaps $\beta = 0.7$ for the 1LIA.

In summary: the behaviour of the measured quantities is much better compatible with scaling if the lattice $\bar{\beta}$ -function is not fixed to the universal (asymptotic) part $\bar{\beta}_{umiv}$. The $\bar{\beta}$ -function at the smallest measured values of the coupling are nearly equal to $\bar{\beta}_{umiv}$ for TIA and 1LIA but otherwise $\bar{\beta}(g)$ is different from $\bar{\beta}_{umiv}$. Scaling (in general) holds better for the improved actions than for the standard one, but with the present errors it is not possible to distinguish numerically between the quality of scaling for the different actions.

7. Summary and conclusions

We have carried out MC calculations for the 2d O(3) non-linear σ -model with three different actions: the standard action (SA); Symanzik's tree-level improved

TABLE 9
 Numerical values of the $\bar{\beta}(g)$ function (always $-\bar{\beta}$ is given) obtained from eqs. (6.5), (6.9)

$\beta = g^{-1}$	μ_G	$\nu = 4$	$\nu = 6$	$\nu = 8$	$\nu = 10$	$\nu = 12$	$\nu = 14$	$\nu = 16$	$\nu = 18$	$-\bar{\beta}_{\text{univ}}$	
SA	0.9	0.51 ± 0.03	0.32 ± 0.04	0.38 ± 0.04	0.45 ± 0.03	0.48 ± 0.02	0.45 ± 0.02	0.44 ± 0.02	0.46 ± 0.02	0.40 ± 0.02	0.231
	1.0	0.38 ± 0.03	0.43 ± 0.04	0.37 ± 0.03	0.36 ± 0.02	0.38 ± 0.01	0.39 ± 0.01	0.36 ± 0.01	0.35 ± 0.01	0.37 ± 0.02	0.184
	1.1	0.29 ± 0.03	0.28 ± 0.03	0.27 ± 0.02	0.28 ± 0.02	0.27 ± 0.01	0.26 ± 0.01	0.28 ± 0.01	0.26 ± 0.01	0.25 ± 0.01	0.151
	1.2	0.19 ± 0.02	0.164 ± 0.014	0.162 ± 0.007	0.184 ± 0.007	0.181 ± 0.006	0.174 ± 0.006	0.174 ± 0.004	0.181 ± 0.006	0.168 ± 0.006	0.125
	1.3	0.15 ± 0.02	0.145 ± 0.009	0.137 ± 0.005	0.138 ± 0.005	0.145 ± 0.006	0.137 ± 0.006	0.132 ± 0.005	0.138 ± 0.006	0.136 ± 0.005	0.106
1LIA	0.7	0.62 ± 0.07	0.37 ± 0.09	0.58 ± 0.09	0.62 ± 0.07	0.62 ± 0.07	0.55 ± 0.05	0.58 ± 0.03	0.57 ± 0.03	0.49 ± 0.04	0.399
	0.8	0.45 ± 0.06	0.30 ± 0.05	0.30 ± 0.04	0.35 ± 0.03	0.37 ± 0.03	0.40 ± 0.03	0.38 ± 0.02	0.38 ± 0.02	0.38 ± 0.02	0.298
	0.9	0.23 ± 0.05	0.20 ± 0.03	0.23 ± 0.02	0.24 ± 0.01	0.24 ± 0.01	0.26 ± 0.02	0.25 ± 0.02	0.25 ± 0.02	0.24 ± 0.02	0.231
TIA	0.9	0.32 ± 0.03	0.35 ± 0.05	0.37 ± 0.03	0.39 ± 0.04	0.39 ± 0.03	0.38 ± 0.02	0.37 ± 0.03	0.37 ± 0.02	0.39 ± 0.02	0.231
	1.0	0.29 ± 0.03	0.36 ± 0.04	0.29 ± 0.04	0.29 ± 0.03	0.27 ± 0.03	0.30 ± 0.04	0.29 ± 0.03	0.27 ± 0.02	0.28 ± 0.02	0.184
	1.1	0.21 ± 0.04	0.19 ± 0.03	0.21 ± 0.03	0.22 ± 0.02	0.21 ± 0.02	0.20 ± 0.03	0.21 ± 0.02	0.19 ± 0.02	0.20 ± 0.01	0.151
	1.2	0.16 ± 0.06	0.15 ± 0.03	0.14 ± 0.02	0.14 ± 0.02	0.15 ± 0.02	0.15 ± 0.02	0.15 ± 0.01	0.14 ± 0.01	0.15 ± 0.01	0.125

action (TIA) and the 1-loop improved action (1LIA). The 1LIA behaves much better with respect to *asymptotic* scaling. Most likely this is an accident, because Symanzik's improvement is made for mass ratios (scaling in general sense) but not for asymptotic scaling.

Scaling in the general sense is also investigated. The numerically determined values of the lattice $\bar{\beta}$ -function $\bar{\beta}(g)$ agree reasonably well if calculated from different physical quantities (although $\bar{\beta}(g)$ is quite different for the three actions). It is expected that the agreement is better for the improved actions, but within the statistical noise of our MC investigation this is practically invisible.

Another aspect of (general) scaling, namely the restoration of Lorentz-invariance in the energy-momentum dispersion, is found to be considerably better for the 1LIA than for the other two actions. This is presumably due to the off-diagonal terms present in the 1LIA. Lorentz-invariance (in particular also rotation invariance, which we did not investigate in this paper) is a very essential requirement.

In summary: the improved actions have led to a better understanding of MC problems in reaching the continuum limit and established a number of interesting features. MC results [23–25] for the 4d SU(2) TIA indicate possible improvements which are in the spirit of Symanzik's program (asymptotic scaling is not improved, however).

We thank Prof. K. Symanzik for his constant interest and advice.

One of the authors (S.M.) would like to thank all members of the Institut für Theoretische Physik, Universität Heidelberg, for the kind hospitality extended to him.

References

- [1] S K Ma, Phys Rev. Lett 37 (1976) 461,
R Swendson, Phys Rev Lett 42 (1979) 859
- [2] K G Wilson, Cargèse lectures 1979, ed G 't Hooft et al (Plenum, New York, 1980)
- [3] S H Shenker and J Tobochnik, Phys Rev B22 (1980) 4462
J E Hirsch and S H Shenker, Phys Rev B27 (1983) 1736
- [4] K Symanzik, in Mathematical problems in theoretical physics, eds R Schrader et al (Lecture Notes in physics 153, Springer, Berlin, 1982), Nucl Phys B226 (1983) 187
- [5] K Symanzik, Nucl Phys B226 (1983) 205
- [6] G Martinelli, G Parisi and R Petronzio, Phys Lett 114B (1982) 251
- [7] B. Berg, S Meyer, I Montvay and K Symanzik, Phys. Lett 126B (1983) 467
- [8] M. Falcioni, G. Martinelli, M L Paciello, B Taglienti and G Parisi, Nucl Phys B225[FS9] (1983)
- [9] E. Brezin and J Zinn-Justin, Phys Rev B14 (1976) 3110
- [10] B Berg and A Billoire, Nucl Phys B221 (1983) 109, Nucl Phys B226 (1983) 405
- [11] K Binder, in Phase Transitions and Critical Phenomena, eds C Domb and M S Green, vol 5 (Academic Press, New York, 1976)
- [12] G Fox, R Gupta, O Martin and S. Otto, Nucl. Phys B205[FS5] (1982) 188
- [13] M Fukugita and Y Oyanagi, Phys Lett 123B (1983) 71
- [14] R Gupta, preprint, CALT-68-1010 (1983)

- [15] J Shigemitsu and J B Kogut, Nucl Phys B190[FS3] (1981) 365,
R Musto, F Nicodemi and R. Pettorino, Nucl Phys B210[FS6] (1982) 263;
D N Lambeth and H E Stanley, Phys Rev B12 (1975) 5302
- [16] M Luscher, Phys Lett 118B (1982) 391
- [17] A Patkos, Preprint, Eötvös University, July 1983
- [18] Y Iwasaki and T Yoshie, University of Tsukuba, Ibaraki preprint, UTHEP-94 (1982), unpublished
- [19] B Berg, Z Phys C20 (1983) 243
- [20] G Martinelli, G Parisi and R Petronzio, Phys Lett 100B (1981) 485
- [21] B Berg and M Luscher, Nucl Phys B180[FS3] (1981) 412
- [22] Y Iwasaki and T Yoshie, Phys Lett 125B (1983) 201
- [23] S Belforte, G Curci, P Menotti and G P Paffuti, Phys Lett 131B (1983) 423
M Fukugita, T Kaneko, T Niuya and A Ukawa, Phys Lett 130B (1983) 73 and addendum
- [24] B Berg, A Billoire, S Meyer and C Panagiotakopoulos, Phys Lett 133B (1983) 359
- [25] F Gutbrod and I Montvay, preprint, DESY 83-112